Pergamon

Bioorganic & Medicinal Chemistry 7 (1999) 1003–1011

BIOORGANIC & MEDICINAL CHEMISTRY

Towards an Understanding of Drug Resistance in Malaria: Three-dimensional Structure of *Plasmodium falciparum* Dihydrofolate Reductase by Homology Building

Thomas Lemcke,[a] Inge Thøger Christensen[b,§] and Flemming Steen Jørgensen[b,*]

[a]*Institute of Pharmacy, University of Hamburg, Bundesstrasse 45, D-20146 Hamburg, Germany*
[b]*Department of Medicinal Chemistry, Royal Danish School of Pharmacy, Universitetsparken 2, DK-2100 Copenhagen, Denmark*

Received 15 May 1998; accepted 2 October 1998

Abstract—A three-dimensional (3-D) model of dihydrofolate reductase (DHFR) from *Plasmodium falciparum* has been constructed by homology building. The model building has been based on a structural alignment of five X-ray structures of DHFR from different species. The 3-D model of the plasmodial DHFR was obtained by amino acid substitution in the human DHFR, which was chosen as template, modification of four loops (two insertions, two deletions) and subsequent energy minimization. The active site of *P. falciparum* DHFR was analyzed and compared to human DHFR with respect to sequence variations and structural differences. Based on this analysis the molecular consequences of point mutations known to be involved in drug resistance were discussed. The significance of the most important point mutation causing resistance, S108N, could be explained by the model, whereas the point mutations associated with enhanced resistance, N51I and C59R, seem to have a more indirect effect on inhibitor binding.

Introduction

Malaria is one of the most widespread diseases in the world. Each year, more than 100 million people are infected and close to one million die, because they do not receive adequate treatment.[1] Malaria is caused by different parasites of Plasmodium, of which *Plasmodium falciparum* is the most vicious one. It causes Malaria tropica, which, without treatment, is very often lethal for the infected patient. There are a number of effective drugs available that interact in different ways with the biochemical life cycle of the parasite (quinine, chloroquine, primaquine, halofantrine, pyrimethamine and proguanil), but as the parasites rapidly develop permanent resistance against the different subclasses, there is a great urge to develop new and effective drugs.[2]

One of the targets for drugs against malaria is the enzyme dihydrofolate reductase (DHFR). Pyrimethamine and cycloguanil (the active metabolite of proguanil) (Fig. 1) are specific inhibitors of the plasmodial DHFR, which is essential to the DNA synthesis. DHFR is an ubiquitous enzyme and it is a target for the anticancer drug methotrexate as well as the antibacterial trimethoprim. The selectivity is due to selective binding of the drugs to the enzyme in the different species.[3,4] DHFR from various species have sequence identities of 25–40%, but despite the low sequence identity the structural homology is very high and all known DHFR structures are remarkably similar. The secondary structure elements that are conserved in all known DHFR structures comprise a central eight stranded sheet and four helices, flanking the sheet (Fig. 2).[5,6] The active site is a 15 Å deep cleft with a core of mostly hydrophobic residues, and an acidic residue at the bottom (Glu or Asp). X-ray crystallographic studies of DHFR co-crystallized with various substrate analogues have shown that the natural substrate, dihydrofolic acid, is bound via hydrogen bonds and hydrophobic interactions to highly conserved residues in the active site.[5,6]

In protozoa DHFR is part of a bifunctional homodimeric protein, where each monomer comprises a DHFR domain, a junctional peptide and a thymidylate synthase (TS) domain. The two functional domains are homologous to monofunctional DHFR and TS, respectively, but as for the monofunctional counterparts the protozoal DHFR domains display considerably less sequence identity compared to the TS domains. The length of the junctional peptide is variable in the bifunctional proteins ranging from a few residues in *Leishmania major* to almost 100 residues in *P. falciparum*.[7]

Key words: Malaria; dihydrofolate; reductase; homology modelling; *Plasmodium falciparum*; resistance.
*Corresponding author. e-mail: flemming@medchem.dfh.dk
§ Present address: Novo Nordisk A/S, Novo Nnordisk Park, DK-2760 Måløv, Denmark.

0968-0896/99/$ - see front matter
PII: S0968-0896(99)00018-8

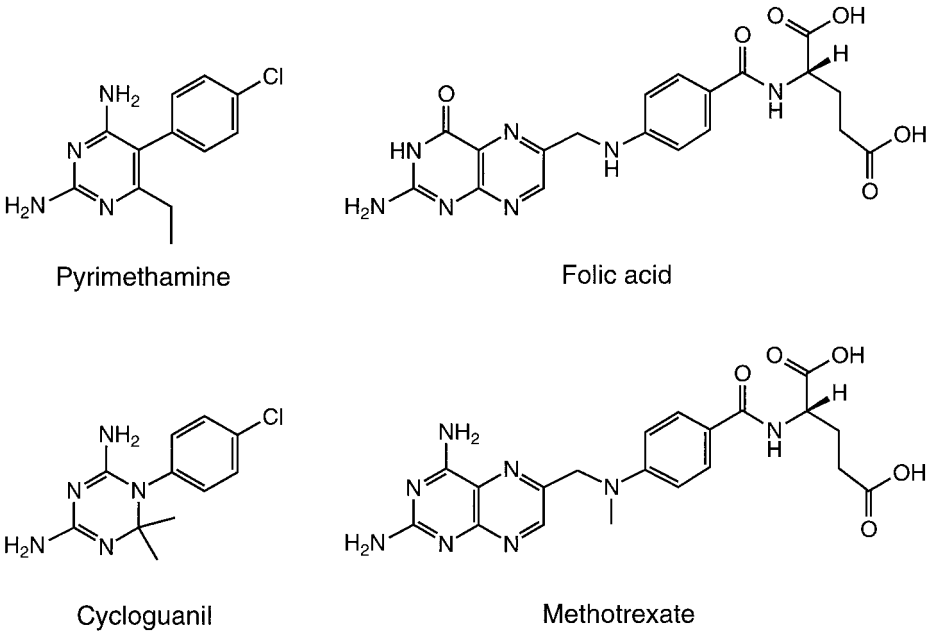

Figure 1. Dihydrofolate reductase inhibitors mentioned in the text.

Figure 2. MOLSCRIPT representation[39] of human DHFR (1drf) illustrating the secondary structure elements.

The 3-D structure of DHFR–TS from *L. major* has been solved by X-ray crystallography,[8] but the coordinates have not yet been made publicly available. According to the authors the two domains display the expected structural similarity to the corresponding monofunctional enzymes. The monomer–monomer interface is very similar to the one found in TS dimers of monofunctional enzymes, and the DHFR–TS interface is determined by the length of the junctional peptide in *L. major*. The N-terminal extension found in protozoal enzymes serves to improve the contacts between the two domains. In contrast to what was predicted in a modelling study,[9] the DHFR domains do not interface each other.

The 3-D structure of plasmodial DHFR is not yet known, but the enzyme is an obvious target for structure-based molecular design. It is of great importance to understand selectivity and resistance at a molecular level in order to be able to design new and more effective antimalarial drugs. Therefore, we have constructed a 3-D model of the plasmodial DHFR, based on sequence and structural alignment of the known 3-D structures of vertebrate and bacterial DHFR.

Methods

The amino acid sequence of *P. falciparum* DHFR (entry C31262)[7] was taken from the NBRF-PIR Database (version 42.0).[10] The coordinates of the 2.0 Å resolution structure of human DHFR (entry 1drf),[11] the 1.7 Å resolution structure of chicken DHFR (entry 8dfr), the 1.9 Å resolution structure of *Escherichia coli* DHFR (entry 3drc),[12] the 1.7 Å resolution structure of *Lactobacillus casei* DHFR (entry 3dfr)[13] and the 2.3 Å resolution structure of *Pneumocystis carinii* DHFR (entry 1daj)[14] were taken from the Protein Data Bank.[15] The sequence alignment of the five protein sequences was carried out using the programme CAMELEON (version 3.12)[16] followed by manual adjustments. Molecular modelling and energy calculations were performed using the SYBYL molecular modelling system (version 6.3).[17] In the energy minimization procedure all hydrogen atoms were included considering a neutral pH for the charged groups. AMBER all-atom partial atomic charges[18] were used for all protein atoms and a dielectric constant of 4 was applied in order to compensate for the lack of water.[19] Energy minimizations were carried out with the MAXIMIN2 minimization algorithm[20] using the SYBYL implementation of the AMBER 3.0 all-atom force field.[21] One to four nonbonded interactions were scaled by a factor of 0.5 and a convergence criterion of 0.005 kcal/mol/Å was applied.

The energy minimization was performed by a stepwise procedure where the protein atoms were gradually relaxed: (1) all sidechain atoms, (2) all sidechains and the backbone of the changed loops and, finally, (3) all atoms. The programmes PROCHECK (version 3.0)[22] and PROSA (version 3.0)[23] were used to evaluate the modelled enzyme structure. Solvent accessible surfaces were calculated using the programme GRID (version 14.0)[24,25] (probe OH2, 0.5 Å grid size).

Results and Discussion

Sequence and structural alignment

The sequences of human, chicken, *E. coli*, *L. casei* and *P. carinii* DHFR were aligned using the programme CAMELEON. Subsequently, the alignment was manually refined by a thorough structural alignment. For this structural alignment the 3-D structures of the chicken, *E. coli*, *L. casei* and *P. carinii* enzymes were fitted to the backbone of the human DHFR (based on the conserved residues Leu27, Gly53, Gly116 of the human enzyme). The conserved secondary structure elements and the regions of significant structural similarity were defined as structurally conserved regions (SCR).[26] The rest of the structure displayed considerable differences in the backbone conformation and were classified as variable regions (VR). The SCRs were then used as a template for the final sequence alignment (Fig. 3).

For the sequence alignment and model building we chose the sequence of the pyrimethamine sensitive 3D7 clone of *P. falciparum*.[27] The sequence was aligned to the structurally derived sequence alignment of the DHFR structures. The alignment was carried out using the programme CAMELEON followed by manual adjustments in order to place insertions and deletions outside structurally conserved regions (Fig. 4). As described by Bzik et al.[7] the amino acid identity between the vertebrates and plasmodium were higher than between the bacteria or fungi and plasmodium (*P. falciparum*–human: 59 residues; *P. falciparum*–*E. coli*: 44 residues; *P. falciparum*–*L. casei*: 37 residues; *P. falciparum*–*P. carinii*: 48 residues). The N-terminal part of the sequence alignment differs from the one published by Bzik et al.,[7] but it is consistent with the more recent alignment based on the 3-D structure of DHFR from *L. major*.[8]

The 3-D structure of the human DHFR was chosen as the template for the model building, because the human and the plasmodial DHFR displayed the highest degree of sequence identity and similarity (59 identical residues = 32%; 87 similar residues = 47%). The first and

Figure 3. Structural alignment of the X-ray crystallographically determined structures of human *Lactobacillus casei*, *Escherichia coli*, chicken and *Pneumocystis carinii* DHFR. The structurally conserved regions are coloured green in all structures, whereas the variable regions are coloured yellow, cyan, and red in vertebrates, bacteria and fungi, respectively.

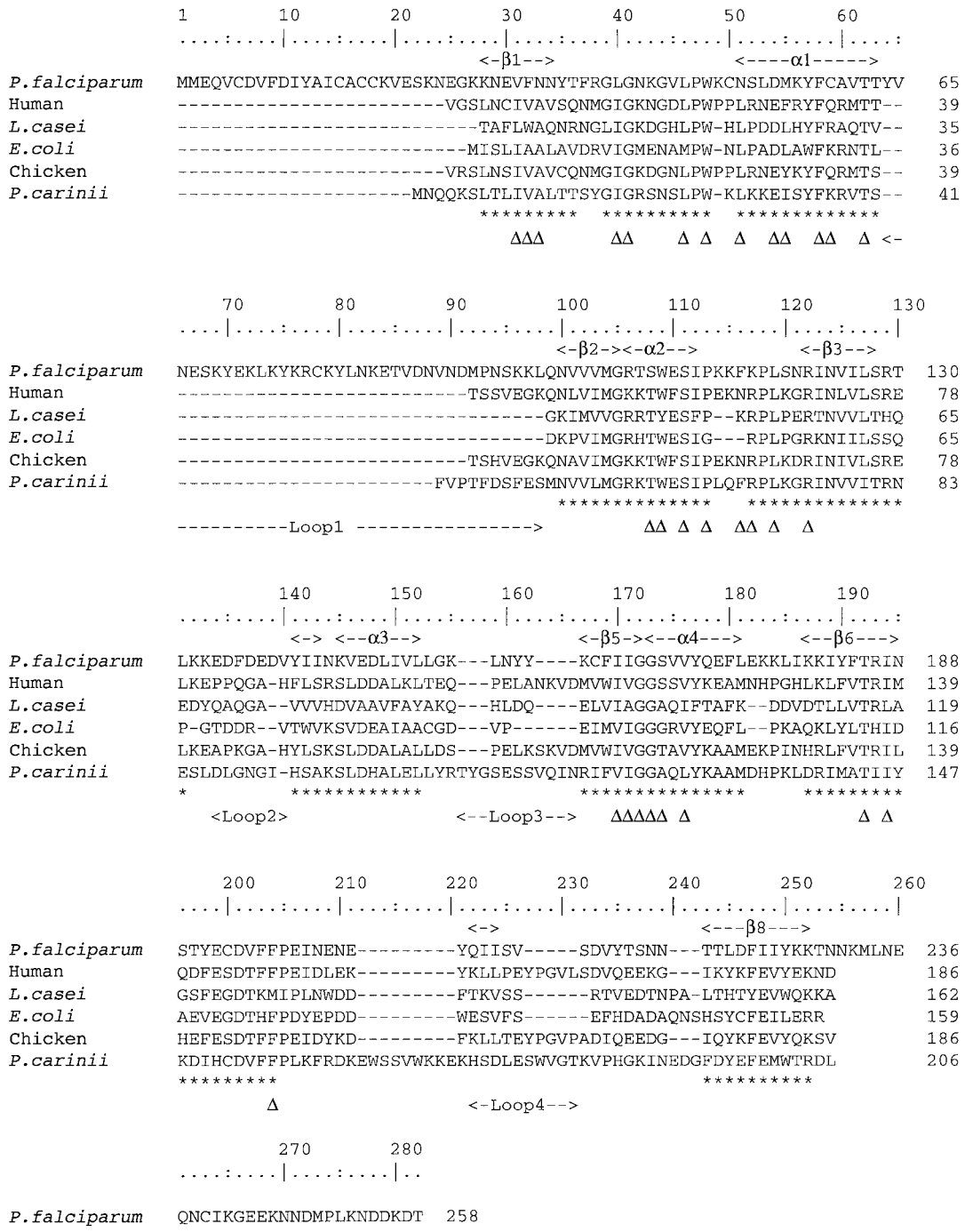

Figure 4. Sequence alignment of *Plasmoduim falciparum* DHFR against the five DHFR with known 3-D structure. The secondary structure elements present in all five 3-D structures are marked above the alignment. The structurally conserved residues and residues lining the substrate binding site are marked by an asterix and a triangle, respectively. The four loops modified during the model building are marked below the alignment.

the last aligned pair of the plasmodial sequence were Glu25 and Asn230, respectively. There was no backbone template for residue 1–24 at the N-terminal and none for residues 231–258 at the C-terminal of the plasmodial sequence. Therefore, no reliable structure could be obtained in these regions. Based on the structural alignment four loop regions, 2 insertions and 2 deletions, were defined. The loops were numbered from 1 to 4 beginning at the N-terminal end (Fig. 4).

Model building

The model building was performed in several steps. In the first step, all amino acids in the SCRs were substituted, using the SYBYL biopolymer module. It leaves the backbone unchanged and replaces the sidechains with new ones. All the sidechain torsion angles ($\chi1,\chi2,\ldots$) are retained where a short sidechain is replacing a long one. In case of a short sidechain being

Table 1. Loops modified in the human DHFR structure during the model building of *Plasmodium falciparum* DHFR. For each loop the original sequence in human DHFR as well as the modified sequence in *P. falciparum* DHFR are listed. The source of the new loop is also listed

Loop[a]	Human DHFR sequence	*P. falciparum* DHFR sequence	PDB entry[b]
1(#40–46)	TSSVEGK	YVNESKYEKLKYKRCKYLNKETVDNVNDMPNSKKL	1prc:H:Pro136-Asp170
2(#82–87)	PPQGAH	EDFDEDV	2apr:Ala202-Thr208
3(#100–110)	TEQPELANKVD	LGKLNYY	1lap:Ala346-Lys352
4(#157–166)	KLLPEYPGVL	QIISV	8cat:Pro308-Val312

[a]Numbering according to human DHFR.
[b]1prc: Photosynthetic reaction center from *Rhodopseudomonas viridis*.[28] 2apr: Acid proteinase from *Rhizopus chinensis*.[36] 1lap: Bovine leucine aminopeptidase.[37] 8cat: Beef liver catalase.[38]

changed to a longer one, the conformation of the new sidechain is taken from a library of preferred sidechain conformations.

The second step involved modelling of the four loops, which was carried out using the loop search facility of SYBYL. Three Cα-carbons, two preceding and one following the loop, were used as anchor points for each loop search. Initially, all loop searches were done independently and the resulting loops were carefully evaluated, considering: (1) homology score, (2) position and orientation of the carbonyl groups in the three anchor residues, (3) root-mean-square (RMS) distances between the Cα-carbons in the anchor residues, and (4) possible collisions with the remaining part of the protein. Finally, the loop searches were carried out in an order that took the changes of the preceding loop search into account and the promising candidates of the first run were tested for possible collisions with other newly found loops. The loop searches were performed in order of increasing complexity: loop2, loop3, loop4, loop1 (Table 1 and Fig. 4). Especially, loop1 was complicated because it involved an insertion of 28 residues. Many of the suggested loops were pointing completely away from the enzyme surface. The selected loop had a good sequence homology score, fitted to the enzyme surface and did not collide with the remaining part of the protein.

In the X-ray structure of human DHFR the residues Asn126-His127-Pro128-Gly129-His130 make the connection between the fourth α-helix and the sixth strand of the β-sheet. According to the alignment the corresponding sequence in the plasmodial enzyme is Glu175-Lys176-Lys177-Leu178-Ile179 and a glycine is, therefore, to be replaced by a leucine. In the human X-ray structure Gly129 is adopting a conformation which is only allowed for glycines, but as the sequence of the chicken enzyme (Glu126-Lys127-Pro128-Ile129-Asn130) is more similar to the plasmodial in this region, the backbone conformation of residues Glu126:Asn130 was adopted from the X-ray structure of chicken DHFR (8dfr) (Fig. 4).

In the third step a short local energy minimization was carried out for each of the carbonyl groups in the anchor residues in order to optimize the junctional regions between loop and protein. A visual inspection of the model built structure and the use of the programme PROCHECK revealed four very close contacts (distances < 1.5 Å). These close contacts were relieved by using the fix_sidechain command of the biopolymer module within SYBYL and by manually adjusting torsion angles of the sidechains within the regions of preferred sidechain conformation. By this procedure a good starting geometry for the energy minimization was obtained. The model building was completed by a stepwise energy minimization of the plasmodial DHFR as described in Methods.

Evaluation

In order to establish the quality of the final energy minimized model structure, the programme PROCHECK was used. Seventy-one percent of the amino acids were located in the most favoured regions of the Ramachandran plot (Fig. 5). Two residues (Lys76 and Asp137) were located in disallowed regions. Lys76 is situated in the first part of loop1 and it was already located in the generously allowed area of the Ramachandran plot in the structure (1prc)[28] retrieved from the PDB. Asp137 is situated on the tip of loop2 and prior to energy minimization this residue is occupying position $i+1$ in a Type II′ -turn ($\Phi,\Psi = 64, -132$). During the energy minimization the loop bends slightly

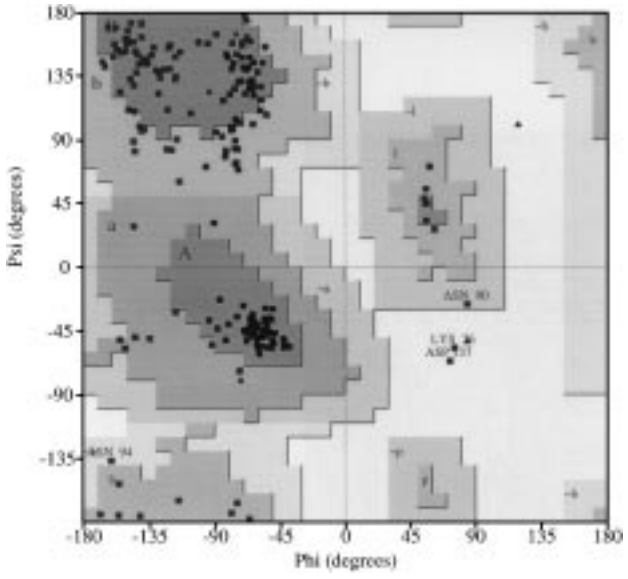

Figure 5. Ramachandran plot produced by PROCHECK of the model build structure of *Plasmodium falciparum* DHFR.

and the conformation changes to a γ-turn having Asp137 in position $i+1$ ($\Phi,\Psi = 72, -67$). The $\chi1-\chi2$ plots (not shown here) revealed good agreement with expected values for sidechains. Bond lengths and hydrogen bond lengths also did not deviate significantly from standard values. Thus, based on the criteria used in PROCHECK, the model built structure could be characterized as a good structure (overall average G-factor −0.10).

The technique of calculating energy profiles based on knowledge based mean fields has successfully been applied to identify protein structures or segments of protein structures, which were misfolded.[23] We have used the PROSA programme to calculate energy profiles for our model built structure of *P. falciparum* DHFR. The profile (not shown here) clearly showed that the part of the structure made up by loop1 was not optimally folded, whereas the remaining part of the structure displayed a z-score or mean force energy well below zero, thus indicating that the overall fold of the *P. falciparum* structure is correct. For loop1 several different loops suggested by the loop search facility in SYBYL were evaluated, but none of these afforded better energy profiles in PROSA than the one originally selected. Considering the length of the loop, it is not surprising that this part of the structure cannot be modelled with the same high degree of reliability as the remaining part of the structure. Thus, even though we took special care in selecting suitable candidates, the conformation of loop1 is still in a way arbitrary. Since the loop is located on the surface of the protein and well away from the cleft, where the active site is located and the area where the co-factor binds, this does not change the usefulness of our model for further investigations of substrate binding, selectivity and building up of resistance (Fig. 6).

Finally, the 3-D structure of our model of plasmodial DHFR was compared to the X-ray structure of the human DHFR. The comparison focused on the structurally conserved regions and particularly on the active site. Except for the modified loops, no major differences between the human DHFR and the plasmodial model DHFR were observed (Fig. 6). This was confirmed by low RMS distances and very good superpositions of the structures (Table 2). Generally, the RMS distances for the active site residues were smaller than for the SCRs, which may indicate that the active sites are less flexible or structurally more conserved.

Active site

The shape of the active site in the *P. falciparum* model was compared to the experimentally determined structures. The programme GRID was used to contour the surface of the active site cleft by calculating the solvent accessible surface. In GRID a 3-D grid is placed around the protein and in each grid point the energy of interaction between the protein and a probe (in this case water) is calculated. The overall shape of the active site

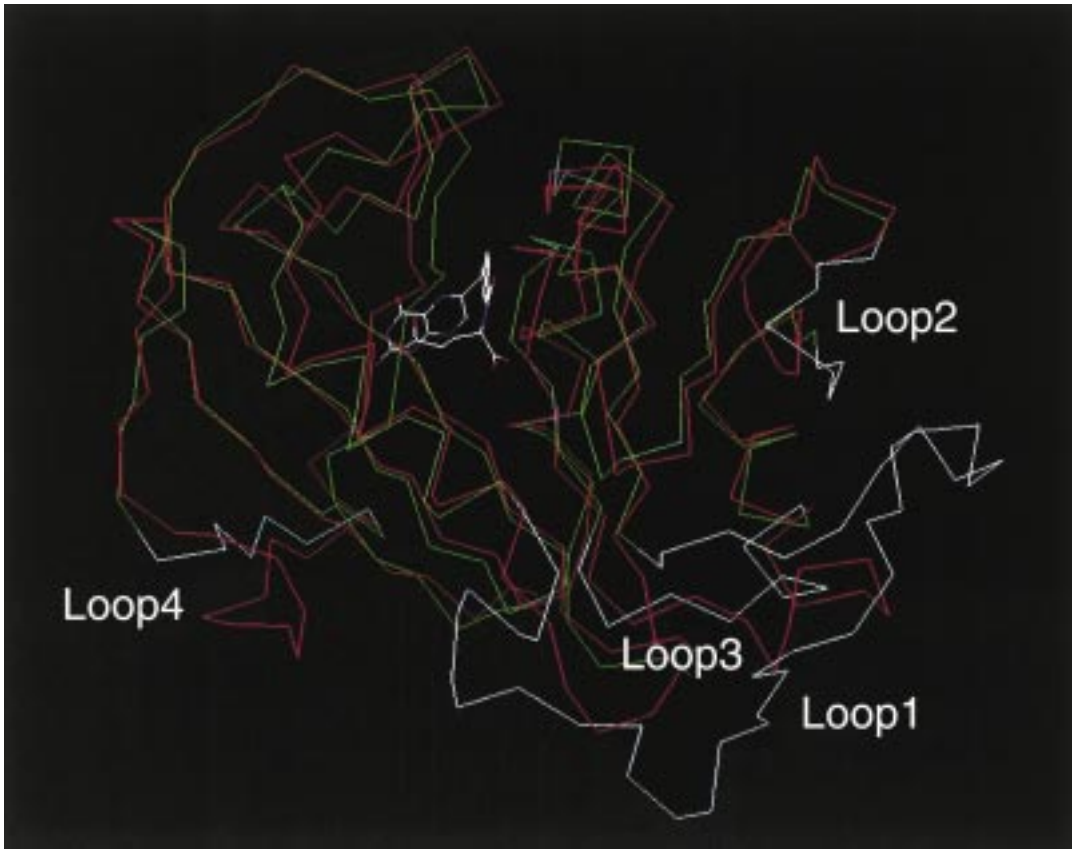

Figure 6. Cα-plot of the energy minimized structure of *Plasmodium falciparum* (green except for the four loops, which are colored cyan) and the X-ray crystallographically determined structure of human DHFR (red). The substrate analogue folic acid present in the human DHFR structure is shown

Table 2. RMS distances[a] between Cα atoms in the 3-D structures of *Plasmodium falciparum*, human, *Lactobacillus casei*, *Escherichia coli*, chicken and *Pneumocystis carinii* DHFR. (SCR, lower left; active site residues, upper right)

	P. falciparum[c]	Human[b]	*L. casei*[b]	*E. coli*[b]	Chicken[b]	*P. carinii*[b]
P. falcipaurm[c]	–	1.06	1.46	1.39	1.20	1.39
Human[b]	1.05	–	0.92	1.10	0.61	0.83
L. casei[b]	1.76	1.35	–	1.09	0.75	0.61
E. coli[b]	1.68	1.46	1.27	–	0.97	0.98
Chicken[b]	1.12	0.50	1.26	1.41	–	0.67
P. carinii	1.54	1.08	1.03	1.26	1.00	–

[a]All values in Å.
[b]X-ray structure.
[c]Homology model, this work.

of *P. falciparum* was retained relative to the human template structure and it was comparable to the shape of the active sites in the other DHFR structures. The substrate analogue folic acid could easily be accommodated in the active site of *P. falciparum* in the same conformation as in the human enzyme (Fig. 7). Thus, the pteridine ring is forming a bidentate hydrogen bond to a carboxylate sidechain (Asp54 in *P. falciparum* and Glu30 in human DHFR) and the proximal carboxylate in the glutamic acid part form a salt bridge to Arg122 and Arg70 in *P. falciparum* and human DHFR, respectively. The most pronounced difference is observed at the entrance to the active site, as the replacement of Asn64 in human DHFR with Phe116 in *P. falciparum* DHFR prevents the enzyme in donating a hydrogen bond to the carbonyl oxygen of the benzoic acid moiety. The residue is found in a variable region just after the highly conserved second α-helix and it must, therefore, be concluded that the hydrogen bond is not essential to substrate binding. Only in vertebrates an asparagine forms this hydrogen bond while in protozoa and fungi there is a conserved phenylalanine at this position. In bacteria a two or three residue deletion is found and no residue can be unambiguously aligned to Asn64. In *L. casei* Lys51 has the potential of donating a hydrogen bond, but sidechain atoms beyond Cβ have not been determined in the X-ray structure (3dfr) and, therefore, it is most unlikely that a hydrogen bond is formed. In the *P. falciparum* model the sidechain of Phe116 adopts a conformation similar to the conformation of the corresponding Phe69 in *P. carinii* making van der Waals contacts to the benzene ring of folic acid.

The substrate binding site of DHFR is lined by 30 residues (Fig. 4). Throughout the six sequences aligned during the model building, 10 residues are identical and an additional 14 represent conservative mutations. Of the remaining 6 only 4 differ between human and *P. falciparum* DHFR. Apart from the Asn64/Phe116 exchange mentioned above the most pronounced difference is Asn33, which makes close contacts to folic acid. This residue is an alanine in most DHFR sequences, but two exceptions are known: in bacteriophage T4[29] it is an aspartic acid and in *P. chabaudi*[30] it is a serine. The remaining two residues, Asn51 and Cys59, display a remarkable sequence variation between the different species. The polar Asn51 corresponds to a non-polar leucine in most other sequences, whereas the non-polar Cys59 corresponds to a polar (glutamine, arginine or lysine) residue.

One of the apparently conservative changes in the active site of *P. falciparum* DHFR is Ser108, which is a threonine in many cases. This residue is, however, biologically very interesting because it is reported to be related to building up of drug resistance against pyrimethamine.[31,32] The S108N point mutant of plasmodial DHFR is catalytically active, but the sensitivity to pyrimethamine is considerably reduced. Ser108, which is directly facing the active site cavity, is unique to pyrimethamine sensitive parasites. Thus, Ser108 may be essential for the activity of pyrimethamine as well as for the sensitivity towards the drug. The resistance to pyrimethamine is further enhanced by point mutation of the above mentioned Asn51 and/or Cys59. These two residues are situated in an α-helix close to the entrance of the active site. It is here interesting to notice the difference between mutations of Ser108 and Asn51/Cys59. The resistant S108N mutant differs more from sequences from other species, having a threonine at the equivalent position, than the pyrimethamine sensitive strains. In contrast, the N51I and C59R mutations cause the *P. falciparum* sequence to converge towards the pattern (a hydrophobic residue in position 51 and a large hydrophilic residue in position 59) common in most sequences.[9]

Various inhibitors containing a diaminopyrimidine moiety have been co-crystallized with DHFR from different species and it has been found that the heterocyclic ring either binds as the 2-amino-4-hydroxy-pteridine ring of folic acid or as the diaminopteridine ring of methotrexate.[33] Assuming that pyrimethamine binds to plasmodial DHFR in a way similar to methotrexate (bidentate contact to Asp54 and hydrogen bonds to backbone groups of Val31 and Ile116), we have docked low energy conformations of pyrimethamine into the active site of our plasmodial DHFR model. In all the available X-ray structures of DHFR-inhibitor complexes the inhibitors adopt folded conformations when bound to the enzyme, but in pyrimethamine the two aromatic ring systems are linearly arranged. If pyrimethamine binds as suggested, the phenyl ring of the inhibitor will be located in a region of the active site that due to the Thr/Ser exchange display noticeable differences between the human and the plasmodial structure (Fig. 7). In the modelled complex pyrimethamine is

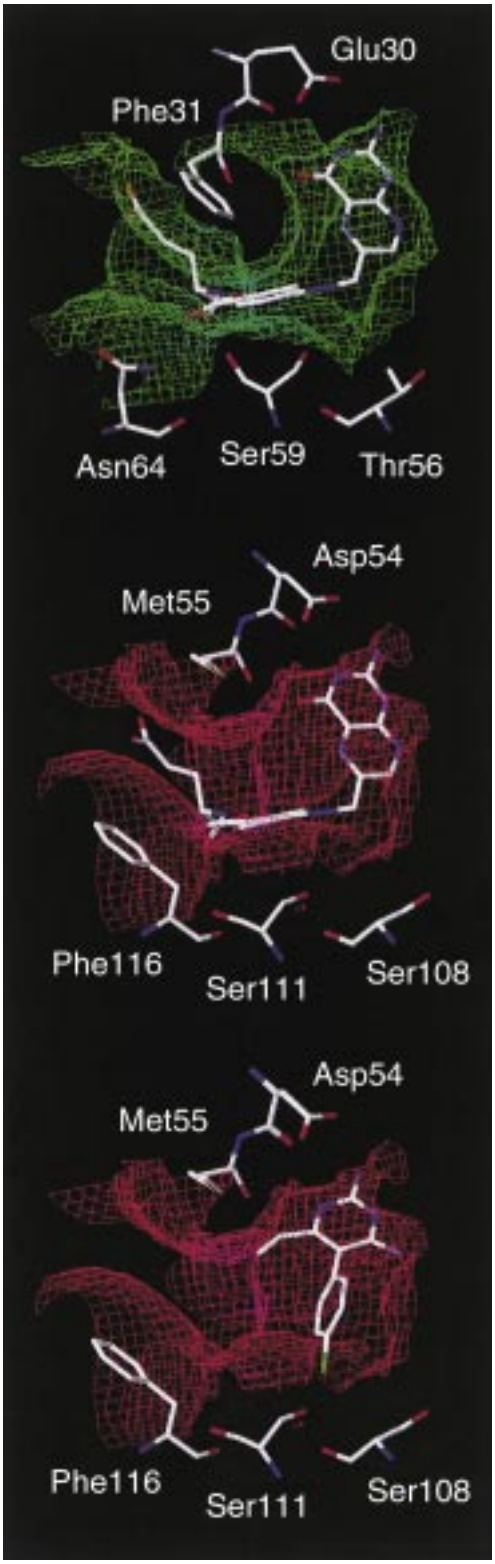

Figure 7. Solvent-accessible surfaces calculated by GRID (water probe, contoured at 0 kcal/mol) of the X-ray crystallographically determined structure of human DHFR (green) and the energy minimized structure of *Plasmodium falciparum* DHFR (red). The substrate analogue folic acid present in the human DHFR structure (1drf) and folic acid and pyrimethamine docked in the *P. falciparum* DHFR model are shown as stick models. Key residues are displayed (see text for further details).

adopting a conformation almost identical to what is found for the X-ray crystal structure of the monoacetylated derivative.[34] The preliminary docking experiments seem to indicate that the chlorine atom in pyrimethamine is in van der Waals contact with Ser108 and Ser111. Consequently, if Ser108 is changed to another residue (e.g. asparagine) there might not be enough space for the inhibitor to bind to the enzyme. This observation is consistent with the reported pyrimethamine resistance of the S108N mutant, and the recently published activity of the meta–chloro isomer of pyrimethamine.[35] The sidechains of Asn51 and Cys59 are not in direct contact with pyrimethamine but they may have an indirect influence on the steric or electrostatic properties of the binding site. Thus, it remains to be shown how the N51I and C59R mutations influence the sensitivity towards pyrimethamine.

Conclusion

A 3-D model of the DHFR-domain from *P. falciparum* has been obtained by homology building. The model was based on the X-ray structure of the human DHFR and a structural alignment of five DHFR structures. Based on the model we were able to explain the significance of the S108N point mutation in relation to pyrimethamine resistance. The dramatically enhanced resistance caused by the N51I and C59R mutations still cannot be explained on a molecular level, and further investigations are required.

The model presented here should be considered as a tool for explaining the mode of action of DHFR antimalarials in general but it will also be a prerequisite for the understanding of species selectivity. Further docking experiments with different inhibitors may allow us to rationalize the structure–activity relationships of antimalarial DHFR inhibitors and, hopefully, to determine the structural requirements for new and more effective inhibitors.

Acknowledgements

This work was supported by a grant from the Danish Medical Research Council. The authors are grateful to Tripos Associates for the support in connection with our use of SYBYL.

References and Notes

1. Implementation of the Global Strategy for Health for All by the Year 2000. Second Evaluation. Eighth Report on the World Health Situation. World Health Organization, Geneva, 1993.
2. Murray, M. C.; Perkins, M. E. *Ann. Rep. Med. Chem.* **1996**, *31*, 141.
3. Burchall, J. J.; Hitchings, G. H. *Mol. Pharmacol.* **1965**, *1*, 126.
4. Ferone, R.; Burchall, J. J.; Hitchings, G. H. *Mol. Pharmacol.* **1969**, *5*, 49.
5. Kuyper, L. F. In *Computer-Aided Drug Design. Methods and Applications*; Perun, T. J.; Propst, C. L.; Eds., Marcel Dekker, New York 1989, Chapter 9, pp. 327–369.

6. Kuyper, L. F. In *Protein Design and the Development of New Therapeutics and Vaccines*; Hook, J. B.; Poste, G.; Eds. Plenum Press, New York 1990, Chapter 15, pp. 297–327.
7. Bzik, D. J.; Li, W.-B.; Horii, T.; Inselburg, J. *Proc. Natl. Acad. Sci. USA* **1987**, *84*, 8360.
8. Knighton, D. R.; Kan, C.-C.; Howland, E.; Janson, C. A.; Hostomska, Z.; Welsh, K. M.; Matthews, D. A. *Struct. Biol.* **1994**, *1*, 186.
9. McKie, J. H. *Drug Des. Discov.* **1994**, *11*, 269.
10. Barker, W. C.; George, D. G.; Hunt, T. L. *Methods Enzymol.* **1990**, *183*, 31.
11. Oefner, C.; D'Arzy, A.; Winkler, F. K. *Eur. J. Biochem.* **1988**, *174*, 377.
12. Warren, M. S.; Brown, K. A.; Farnum, M. F.; Howell, E. E.; Kraut, J. *Biochemistry* **1991**, *30*, 11092.
13. Bolin, J. T.; Filman, D. J.; Matthews, D. A.; Hamlin, R. C.; Kraut, J. *J. Biol. Chem.* **1982**, *257*, 13650.
14. Cody, V.; Galitsky, N.; Luft, J. R.; Pangborn, W.; Gangjee, A.; Devraj, R.; Queener, S. F.; Blakley, R. L. *Acta Crystallogr., Sect. D* **1997**, *53*, 638.
15. Bernstein, F. C.; Koetzle, T. F.; Williams, G. J. B.; Meyer, E. F., Jr.; Brice, M. D.; Rodgers, J. R.; Kennard, O.; Shimanouchi, T.; Tasumi, M. *J. Mol. Biol.* **1977**, *112*, 535.
16. Oxford Molecular Ltd., Oxford, UK.
17. Tripos Associates Inc., St. Louis, USA.
18. Weiner, S. J.; Kollman, P. A.; Nguyen, D. T.; Case, D. A. *J. Comput. Chem.* **1986**, *7*, 230.
19. Christensen, I. T.; Jørgensen, F. S. *J. Biomol. Struct. Dyn.* **1997**, *15*, 473.
20. Labanowski, J.; Motoc, I.; Naylor, C. B.; Mayer, D.; Dammkoehler, R. A. *Quant. Struct.-Act. Relat.* **1986**, *5*, 138.
21. Weiner, P. K., Kollman, P. A. *J. Comput. Chem.* **1981**, *2*, 287.
22. Morris, A. L.; MacArthur, M. W.; Hutchinson, E. G.; Thornton, J. M. *Proteins* **1992**, *12*, 345.
23. Sippl, M. J. *Proteins* **1993**, *17*, 355.
24. Boobbyer, D. N. A.; Goodford, P. J.; McWhinnie, P. M.; Wade, R. C. *J. Med. Chem.* **1989**, *32*, 1083.
25. Goodford, P. J. *J. Med. Chem.* **1985**, *28*, 849.
26. Greer, J. *Proteins*. **1990**, *7*, 317.
27. Cowman, A. F.; Morry, M. J.; Biggs, B. A.; Cross, G. A. M.; Foote, S. J. *Proc. Natl. Acad. Sci. USA* **1988**, *85*, 9109.
28. Deisenhofer, J.; Epp, O.; Sinning, I.; Michel, H. *J. Mol. Biol.* **1995**, *246*, 429.
29. Purokit, S.; Mathews, C. K. *J. Biol. Chem.* **1984**, *259*, 6261.
30. Cowman, A. F.; Lew, A. M. *Mol. Cell. Biol.* **1989**, *9*, 5182.
31. Peterson, D. S.; Walliker, D.; Wellems, T. E. *Proc. Natl. Acad. Sci. USA* **1988**, *85*, 9114.
32. Sirawaraporn, W.; Sathitkul, T.; Sirawaraporn, R.; Yathavong, Y.; Santi, D. V. *Proc. Natl. Acad. Sci. USA* **1997**, *94*, 1124 and references therein.
33. Blakley, R. L. *Adv. Enzymol. Relat. Areas Mol. Biol.* **1995**, *70*, 23 and references therein.
34. Griffin, R. J.; Lowe, P. R. *J. Chem. Soc., Perkin Trans. 1*, **1992**, 1811.
35. McKie, J. H.; Douglas, K. T.; Chan, C.; Roser, S. A.; Yates, R.; Read, M.; Hyde, J. E.; Dascombe, M. J.; Yuthavong, Y.; Sirawaraporn, W. *J. Med. Chem.* **1998**, *41*, 1367.
36. Suguna, K.; Bott, R. R.; Padlan, E. A.; Subramanian, E.; Sheriff, S.; Cohen, G. H.; Davies, D. R. *J. Mol. Biol.* **1987**, *196*, 877.
37. Burley, S. K.; David, P. R.; Taylor, A.; Lipscomb, W. N. *Proc. Natl. Acad. Sci. USA* **1990**, *87*, 6878.
38. Fita, I.; Rossmann, M. G. *Proc. Natl. Acad. Sci. USA* **1985**, *82*, 1604.
39. Kraulis, P. J. *J. Appl. Cryst.* **1991**, *24*, 946.